Front. Earth Sci. 2013, 7(3): 351–360
DOI 10.1007/s11707-013-0366-y

RESEARCH ARTICLE

Impacts of river impoundment on the riverine water chemistry composition and their response to chemical weathering rate

Yang GAO[1], Baoli WANG[2], Xiaolong LIU[3], Yuchun WANG[4], Jing ZHANG[1], Yanxing JIANG[1], Fushun WANG (✉)[1]

1 School of Environmental and Chemical Engineering, Shanghai University, Shanghai 200444, China
2 Institute of Geochemistry, Chinese Academy of Science, Guiyang 550002, China
3 Tianjin Normal University, Tianjin 300387, China
4 Department of Water Environment, China Institute of Water Resources and Hydroelectric Power Research (IWHR), Beijing 100038, China

Abstract Currently, most rivers worldwide have been intensively impounded. River damming becomes a big problem, not only in inducing the physical obstruction between upstream and downstream, but also in destroying the natural continuity of river. But the discontinuity of water quality was often neglected, which presents a challenge to traditional river geochemistry research. To understand the changes in basic chemistry of water upstream and downstream of the dam, we investigated the Miaotiao River reservoirs in series in the Wujiang River Basin, and the Hongjiadu, Dongfeng Reservoir on the upper reaches of the Wujiang River. Chemical weathering rates were calculated using the water chemistry data of the reservoir surface and downstream of the dam, in each reservoir, respectively. The results showed that the difference between the chemical weathering rates calculated from reservoir surface water and water downstream of the dam was greater in reservoirs with a longer water retention time. In Hongjiadu Reservoir with the longest water retention time among the studied reservoirs, this difference reaches 9%. As a result, the influence of river damming, especially the influence of reservoirs in series, should be taken into account when calculating the chemical weathering rate of a river basin.

Keywords reservoirs in series, chemical weathering rate, Wujiang

1 Introduction

During the past century, river impoundment has become a popular hydrological landscape imposed on rivers worldwide. Globally, there are more than 50 thousand big dams (height of dam over 15 m, or storage over 3.0×10^6 m^3), and 100 thousand small reservoirs with storage over 10^5 m^3, and millions of smaller reservoirs (storage less than 10^5 m^3). The effective storage of the global reservoir is about 4×10^{12} m^3, and about 7.3% of the annual discharge of global rivers. The total area of reservoirs in the world is 5×10^5 km^2, about 1/3 that of natural lakes. In China, till 2007, more than 86,000 reservoirs have been constructed with a total storage of 6.9×10^{11} m^3 (Jia et al., 2010).

A natural stream is a continuous system which connects the headwater of a river to the river mouth or coastal zone. However, the natural properties and biogeochemical processes of rivers have been seriously disturbed by human activities, of which river damming can be regarded as the most important of human affairs imposed on a river system. Numerous dams on a river are not only the physical obstruction between water upstream and downstream the dam, but they also can destroy the natural continuity of the river. As a result, water quality as well as the hydrological property of river are often very different upstream and downstream of the dam. Rivers, hence, show a trend to be lacustrine and fragmental. At present, reservoir effect has been observed in many studies on rivers worldwide, such as the Danube and Nile (Humborg et al., 1997). Sedimentary and geomorphic properties of river channels downstream of dams changed substantially (Yang et al., 2007; Walter and Merritts, 2008; Kummu et al., 2010). The impacts of river damming on hydrological structure, sediment deposition, fish migration and the potential earthquake have long been of concern (Humborg et al., 1997; Dumas et al., 2010; Musil et al., 2012; Zhang et al., 2012). Recently, the changes in river ecosystems, due to the dam construction, were also reported (Dynesius

Received November 26, 2012; accepted February 25, 2013

E-mail: fswang@shu.edu.cn

and Nilsson, 1994). The impacts of dam construction on the riverine biogeochemical processes and the induced ecological issues have been confirmed (Mao et al., 2005; Qi and Ruan, 2005). The relationship between reservoir and ecosystem evolution also has become a great concern (Cai et al., 2003) reduced reservoir reduces the suspended sediment deposition in the downstream reach because upper stream suspended sediment was trapped by the reservoir (Wang et al., 2012). The construction of dams can intercept upstream sediment and fundamentally change the fluvial hydrology (Kiss et al., 2008; Draut et al., 2011). Undoubtedly, large-scale river damming can significantly change the riverine material field, energy field, chemical field, and biological field, as well as the hydrodynamic regime.

In addition to the above environmental impacts, geochemical processes happening in reservoirs also can change the river water chemistry. For instance, it was reported that carbon could be obviously retained within a reservoir due to river impoundment, and riverine water chemistry characteristics also had a significant change (Li et al., 2009). However this variation of water chemistry gradually challenges the accurate evaluation of chemical weathering rate (CWR). In traditional chemical weathering research, changes in water chemical composition within a river channel were seldom considered (Brink et al., 2007; Wu et al., 2008; Moquet et al., 2011), which may bring an uncertain deviation of the CWR results. In this study, the reservoirs in series in the Miaotiao River and the Hongjiadu Reservoir, the Dongfeng Reservoir on the upper reaches of the Wujiang River were investigated. The main objectives are to quantify the changes in basic water chemistry upstream and downstream of the dam, and to understand their influence on CWR calculation.

2 Study area

The Wujiang River, originating from north-west of Guizhou Province, China, is an important tributary of Changjiang. The Maotiao River, developed in a karstic area, is an important tributary of the Wujiang River. The Maotiao River has a total length of 180 km, and drains an area of 3195 km^2. The middle and lower reaches of the Wujiang River have developed into deep canyons, which have always been exploited for hydropower generation.

The altitudes of the Wujiang River watershed are about 1500 m in its upper reach and about 500 m in its lower reach. Precipitation in this basin has a yearly average of 1225 mm.

Since the construction of the Wujiangdu Reservoir, twelve hydropower plants in series were built on the Wujiang River successively, of which, six reservoirs are on the major tributary (Maotiao River). In this study, four reservoirs on the main-stream of the Wujiang River (Wujiangdu(WJD), Dongfeng(DF), Suofengying(SFY) and Hongjiadu(HJD)) and four reservoirs(Hongfeng(HF), Baihua(BH), Xiuwen(XW) and Hongyan(HY)) on the Maotiao River were investigated. The main features of these reservoirs are described in Table1.

3 Sampling and methods

3.1 Sampling

In each reservoir, water was collected before and after the dam monthly from July 2007 to June 2008. The site before the dam is about 500 m from the dam, and the site after the dam is the downstream side of the dam. Sampling sites are shown in Fig. 1. Samples downstream of the dam were collected 0.5 m under the water surface, while water samplings along the water column were collected in the central part of the reservoir using a Niskin bottle.

Water temperature, dissolved oxygen (DO) saturation, and pH were measured at the sampling sites with a pH, DO and salt conductivity meter (YSI-6600v2). HCO_3^- was titrated by HCl in situ. All water samples were filtered through 0.45 μm acetate membrane filters and a small portion of filtrate was stored in the icebox for measuring anions, while another portion was acidified with ultra-purified hydrochloric acid to pH < 2 for cation determina-

Table 1 Main features of studied reservoirs

Reservoir	Drainage area/km^2	Average flow /(m^3·s^{-1})	Average annual precipitation/mm	Total volume / (10^{8}m^3)	Year of construction	Height of dam/(m^{-1})	Residence time/d
Hongfeng	1551	30.2	1584.95	6.01	1960	54	230.3
Baihua	1832	38	1362.4	1.82	1974	50	55.4
Xiuwen	2084	41.2	1230.7	0.114	1961	49	3.2
Hongyan	2752	49.2	1108	0.304	1971	60	7.2
Hongjiadu	9900	155	1191.4	49.47	2000	182	568.5
Dongfeng	18161	343	1118.3	8.64	1984	162	54.35
Suofengying	21862	395	1061.2	2.012	2001	113	4.9
Wujiangdu	27790	483	1124.7	23	1970	165	82.5

Note: The above data of drainage area, average flow, average annual precipitation, total volume, construction year and Height are from the hydrological yearbooks of China and www.data.ac.cn, the Residence time = total volume/average flow

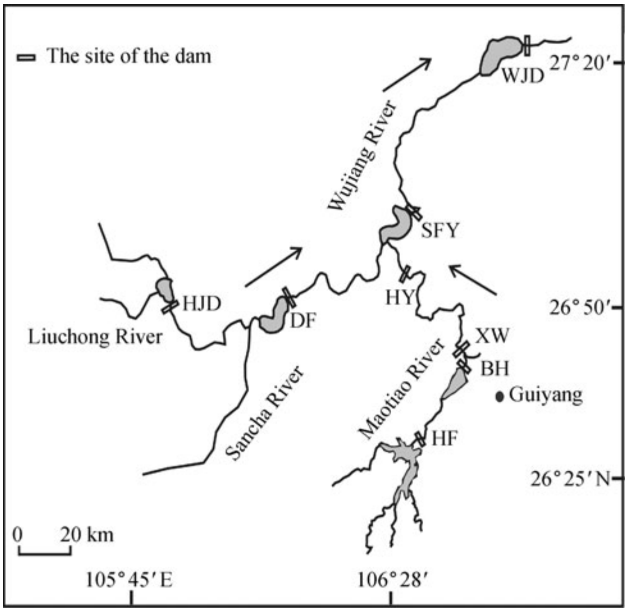

Fig. 1 Geographic location of study area and sampling sites

tion. Major cations (Ca^{2+}, K^+, Na^+ and Mg^{2+}) were analyzed by ICP-OES, and the anions (SO_4^{2-}, Cl^- and NO_3^-) by ion chromatography (ICS-90, DIONEX). Dissolved Si was measured by silicon molybdenum blue spectrophotometry. Repeat measurements show that in general the precision is ±2% for cations and ±5% for anions. Data in Table 2 is the annual average of the monthly monitoring data. TZ^+ refers to the total cation concentration. TZ^- is the total anions concentration.

3.2 Methods

3.2.1 The chemical weathering rate (CWR) calculation process

Step 1: Atmospheric correction

This step assumes that all of the major elements from atmospheric sources remain in the river water.

$$FX_{cycl} = FX_{atm}. \quad (1)$$

With FX_{cycl} the flux of the element X from atmospheric inputs exported by the river and FX_{atm} the rain flux of the element X

Where

$$FX_{atm} = X_{atm} \times P, \quad (2)$$

$$FX_{cycl} = X_{cycl} \times R. \quad (3)$$

And X_{cycl} is the concentration of the element X in the river derived from atmospheric inputs (mmol/L); X_{atm} is the concentration of the element X in the rain (mmol/L); P is the precipitation rate, and R is the runoff (mm/yr).

The P/R is the ratio of the precipitation and runoff. To determine the cyclic concentration of the major elements X (Cl^-, SO_4^{2-}, Ca^{2+}, Na^+, Mg^{2+}, and K^+) in the river, we applied the following calculation:

$$X_{cycl} = X_{atm} \times P/R, \quad (4)$$

where X_{atm} is the average concentration of the element X from rain data for each area.

In all cases: $HCO_{3\ cycl}^- = Si_{cycl} = 0$ mmol/L.

The residual concentration is calculated following this equation:

$$X_1 = X_{riv} - X_{cycl}, \quad (5)$$

where X = Cl^-, SO_4^{2-}, HCO_3^-, Na^+, Ca^{2+}, Mg^{2+}, and K^+(mmol/L),

$$Si_1 = Si_{riv}, \quad (6)$$

where Si_{riv} is from the silicate weathering.

Step 2: Saltrock, pyrite, and hydrothermal correction

Depending on the basin characteristics, all remaining Cl^- and SO_4^{2-} are assumed to be derived from evaporite dissolution.

$$Cl_{evap}^- = Cl_1^-, \quad (7)$$

$$SO_{4\ evap}^{2-} = SO_{4\ 1}^{2-}, \quad (8)$$

$$Na_{evap}^+ = Cl_{evap}^-(\text{mmol/L}), \quad (9)$$

$$Ca_{evap}^{2+} = SO_{4\ evap}^{2-} \text{ and}$$
$$Mg_{evap}^{2+} = 0\,\text{mmol/L}\ (SO_{4\ evap}^{2-} \text{ is derived from } CaSO_4),$$

where X_{evap} is the X concentration derived from evaporate inputs.

Residual concentration (mmol/L):

$$Na_2^+ = Na_1^+ - Na_{evap}, \quad (10)$$

$$Ca_2^{2+} = Ca_1^{2+} - Ca_{evap}^{2+}, \quad (11)$$

$$Mg_2^{2+} = Mg_1^{2+} - Mg_{evap}^{2+}, \quad (12)$$

$$HCO_{3\ 2}^- = HCO_{3\ 1}^-, \quad (13)$$

$$Si_2 = Si_1. \quad (14)$$

Step 3: Silicate weathering

The silicate inputs are calculated following these equations:

$$Na_{sil}^+ = Na_2^+ \quad (15)$$

Table 2 Water chemistry data of the samples and the CWR of the reservoirs

	HF-1	HF-2	BH-1	BH-2	XW-1	XW-2	HY-1	HY-2	HJD-1	HJD-2	DF-1	DF-2	SFY-1	SFY-2	WJD-1	WJD-2
pH	8.46	7.42	8.37	7.34	7.96	7.46	8.32	7.66	8.12	7.56	8.27	7.73	8	7.78	8.34	7.57
DO/%	93.68	46.59	98.9	47.62	74.86	46.58	126.72	53.54	85.38	64.77	99.84	64.18	95.95	73.79	116.08	87.2
TDS /($mg\cdot L^{-1}$)	279.95	308.2	337.14	380.51	364.15	363.83	330.45	342.33	280.17	302.97	316.88	306.93	314.93	311.56	333.55	327.99
K^+/($mmol\cdot L^{-1}$)	0.068	0.067	0.081	0.076	0.08	0.093	0.081	0.073	0.035	0.038	0.037	0.039	0.042	0.043	0.048	0.045
Ca^{2+}/ ($mmol\cdot L^{-1}$)	1.198	1.365	1.41	1.494	1.574	1.467	1.326	1.37	1.359	1.509	1.485	1.505	1.514	1.508	1.563	1.583
Na^+/($mmol\cdot L^{-1}$)	0.222	0.224	0.382	0.318	0.346	0.483	0.372	0.343	0.15	0.147	0.259	0.194	0.209	0.213	0.22	0.208
Mg^{2+}/ ($mmol\cdot L^{-1}$)	0.666	0.573	0.6	0.588	0.551	0.589	0.649	0.582	0.363	0.36	0.386	0.378	0.418	0.407	0.483	0.454
Cl^-/($mmol\cdot L^{-1}$)	0.174	0.163	0.201	0.178	0.169	0.221	0.192	0.176	0.072	0.073	0.091	0.082	0.09	0.088	0.12	0.099
SO_4^{2-} /(mmol $\cdot L^{-1}$)	0.901	0.943	1.12	1.103	1.109	1.171	0.991	0.956	0.681	0.702	0.936	0.816	0.858	0.846	0.937	0.905
NO_3^- /(mmol $\cdot L^{-1}$)	0.087	0.082	0.068	0.095	0.132	0.125	0.113	0.11	0.242	0.253	0.204	0.23	0.211	0.216	0.179	0.2
HCO_3^- /(mmol $\cdot L^{-1}$)	1.806	2.142	2.221	2.922	2.562	2.431	2.315	2.589	2.12	2.351	2.214	2.233	2.284	2.248	2.412	2.368
Si/ ($mmol\cdot L^{-1}$)	0.007	0.018	0.018	0.02	0.024	0.023	0.022	0.028	0.041	0.067	0.054	0.064	0.058	0.059	0.029	0.058
TZ^+/ ($meq\cdot L^{-1}$)	4.018	4.169	4.483	4.559	4.676	4.687	4.403	4.321	3.629	3.924	4.039	4	4.113	4.087	4.361	4.326
TZ^-/ ($meq\cdot L^{-1}$)	3.87	4.273	4.731	5.401	5.08	5.119	4.601	4.787	3.797	4.081	4.381	4.176	4.3	4.244	4.586	4.477
NICB	0.037	−0.025	−0.055	−0.185	−0.086	−0.092	−0.045	−0.108	−0.046	−0.04	−0.085	−0.044	−0.046	−0.038	−0.052	−0.035
CRWsil/(t$\cdot$ $(km^2\cdot yr)^{-1}$)	3.1	3.82	7.7	6.53	7.44	9.91	6.75	6.47	3.46	4.22	6.95	5.97	5.73	5.95	4.23	5.32
CRWcarb /($t\cdot (km^2\cdot yr)^{-1}$)	52.73	55.29	47.26	54.69	53.59	42.14	45.65	47.35	47.9	54.27	48.17	57.94	55.17	54.83	55.09	56.36
CRWevap /($t\cdot (km^2\cdot yr)^{-1}$)	74.4	77.59	100.32	98.26	94.14	100.54	76.54	73.57	43.49	44.94	74.44	64.5	65.16	64.22	68.9	66.07

Notes: NICB = $(TZ^+ - TZ^-)/TZ^+$; 1. reservor surface; 2. downstream the dam

$$Ca^{2+}_{sil} = Na^{+}_{sil} \times (Ca^{2+}/Na^{+})_{sil}, \quad (16)$$

$$Mg^{2+}_{sil} = Na^{+}_{sil} \times (Mg^{2+}/Na^{+})_{sil}, \quad (17)$$

$$Si_{sil} = Si_{2}, \quad (18)$$

$$K^{+}_{sil} = K^{+}_{2}(\text{mmol/L}), \quad (19)$$

where $(Ca^{2+}/Na^{+})_{sil}$ and $(Mg^{2+}/Na^{+})_{sil}$ are the characteristic ratios of silicates. Previous studies (Han and Liu, 2004; Wu et al., 2005) were used to estimate the composition of the silicate end-member. In following the discussion, Mg/Na and Ca/Na are assumed to be close to 0.22 and 0.35 (Chetelat et al., 2008). The chemical weathering concentration of silicates (CWC_{sil}) is calculated as follows:

$$CWC_{sil} = Na^{+}_{sil} + Ca^{2+}_{sil} + Mg^{2+}_{sil} + K^{+}_{sil} + SiO_{2}(\text{mg/L}). \quad (20)$$

Step 4: Carbonate weathering

Any remaining cations not accounted for by rain, evaporates, or silicates were attributed to carbonate weathering. The chemical weathering concentration of carbonates (CWC_{carb}) is calculated as follows:

$$Ca^{2+}_{carb} = Ca^{2+}_{2} - Ca^{2+}_{sil}, \quad (21)$$

$$Mg^{2+}_{carb} = Mg^{2+}_{2} - Mg^{2+}_{sil}, \quad (22)$$

$$HCO^{-}_{3\ calcite/dolomite} = Ca^{2+}_{carb} + Mg^{2+}_{carb}(\text{mmol/L}), \quad (23)$$

$$CWC_{carb} = Ca^{2+}_{carb} + Mg^{2+}_{carb} + HCO^{-}_{3\ calcite/dolomite}(\text{mg/L}). \quad (24)$$

Step 5: CWR (Chemical weathering rate) calculation

$$CWR_{sil} = CWC_{sil} \times R/a\left(t/(km^{2}\cdot yr)\right), \quad (25)$$

$$CWR_{carb} = CWC_{carb} \times R/a\left(t/(km^{2}\cdot yr)\right), \quad (26)$$

where R is runoff (mm/yr) and a is drainage area (km^2)

3.2.2 $CaCO_3$ saturation index (SIc) calculation method

SIc was calculated from the following Eq. (27):

$$SIc = \lg\left((Ca^{2+})(CO^{2-}_{3})/K_{C}\right), \quad (27)$$

where Kc is the temperature dependent equilibrium constant for calcite dissociation. Ca^{2+} and CO_3^{2-} are measured in mmol/L.

4 Result and discussion

4.1 Variations of major ions composition in river water of the study area

The average pH is 7.9 (with a range of 7.34–8.37) in the Wujiang River, indicating the geological background of limestone in the drainage basin. TDS values vary from 279.9 to 364.1 mg/L, except for a high value (380 mg/L) of the sample (BH) (Table 2), which was polluted by waste water from a nearby aluminum factory.

TZ^+ ($K^+ + Na^+ + 2Ca^{2+} + 2Mg^{2+}$), TZ^+ in meq/L and major element concentration in mmol/L, in river water has a range of 3.63–4.69 meq/L, with a mean value of 4.23 meq/L, which is higher than the average of the world rivers (1.25 meq/L, Meybeck, 1982). Because of draining a karst terrain, the TDS value in the Wujiang River is also higher than the Changjiang River (2.8 meq/L on average) (Han and Liu, 2004).

HCO_3^- is the dominant anion for the majority of the samples (1.8–2.9 mmol/L). The second major anion is SO_4^{2-}, which has an average concentration of 0.93 mmol/L. Cl^- and NO_3^- concentrations ranging from 0.07 to 0.22 mmol/L and from 0.06 to 0.25 mmol/L, respectively. SO_4^{2-} and HCO_3^- together account for 90% of the total anions in river water, while Ca^{2+} and Mg^{2+} together account for 80% of the total cations.

Variations of major ion compositions are shown in the anion and cation ternary diagrams (Figs. 2(a) and 2(b)). It is clear that Ca^{2+} and HCO_3^- are the dominant ions in the water and an indication of the carbonate dissolution. Most of the samples are distributed around the Ca^{2+} apex and the HCO_3^- apex in the ternary anion diagram (Fig. 2), revealing strong carbonate weathering and less silicate weathering in the drainage basin.

4.2 Reservoir effects on CWR evaluation

Our results showed that the difference between the chemical weathering rates calculated from reservoir surface water and water downstream the dam varied between −4.23% and 9.04%, and had a trend to be greater in a reservoir with longer water retention time (Fig. 3). For example, in Fig. 3, it is clear that, the CWR above the dam is similar to the CWR below the dam, in XW, SFY, and HY. However, in BH, HF, and HJD reservoirs, which have a longer water retention time, the CWR showed large differences. Based on these data, a linear relationship between the rate of change and the retention time of reservoirs can be found (Fig. 3).

The rate of change = ((weathering rate below the dam) – (weathering rate before the dam)) / (weathering rate before the dam).

Table 2 shows that the dissolved Si and Ca^{2+} concentration in water downstream the dam were higher,

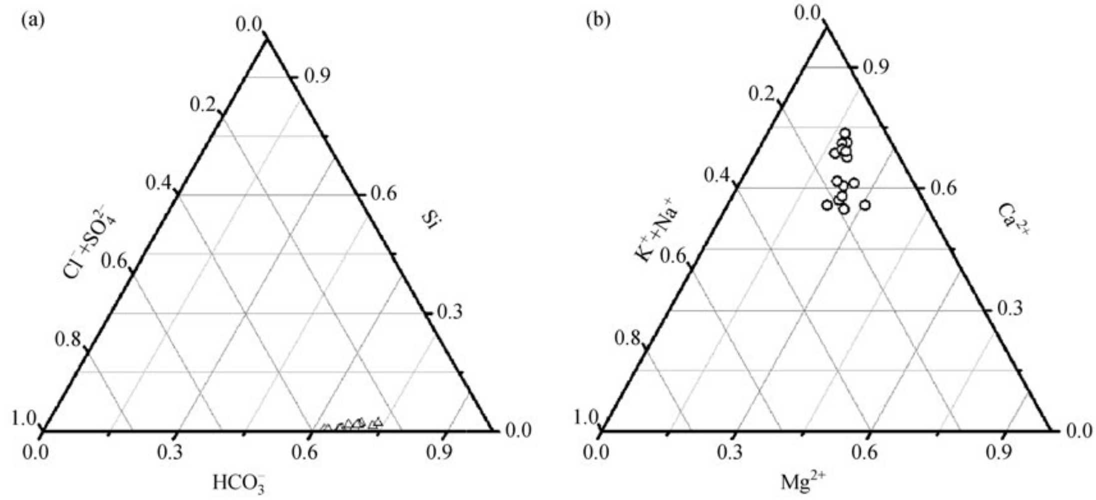

Fig. 2 The anion and cation ternary diagrams

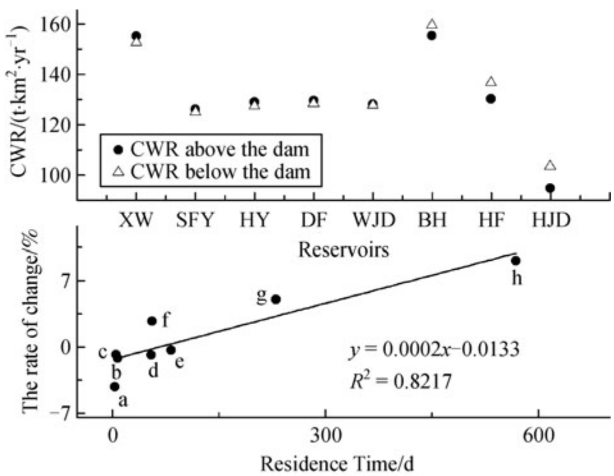

Fig. 3 Relationship between water residence time and changes of CWR (a-XW, b-HY, c-SFY, d-DF; e-WJD, f-BH, g-HF, h-HJD). (The residence times are in Table 1).

compared with the surface water upstream of the dam, in reservoirs with longer residence time. For instance, the dissolved Si concentration in downstream water was two times that of the surface water upstream of the dam in the HF reservoir, and the Ca^{2+} concentration had a variation of 10%–20% (variation rate = ((concentration in downstream) – (concentration in surface water upstream the dam)) / (concentration in surface water upstream the dam)). Compared with Ca^{2+} and Si, the variations of K^+, Cl^-, SO_4^{2-} were small. We conclude that the main factors influencing the CWR calculation should be Ca^{2+} and Si. In addition, because carbonate is dominant in the studied basin, Si has a quite low concentration in the river water. Consequently, the geochemical behavior of Ca^{2+} in the reservoir-river system should be the major contribution to the CWR variation.

4.3 Mechanism for the variation of water chemistry composition in reservoir Lacustrine reaction in reservoir

The water temperatures above and below the dam are shown in Fig. 4. From Fig. 4, the temperature differences above and below the dam are more obvious in the HJD, HF, and WJD reservoirs during warm seasons. This is because these reservoirs have longer residence time, and consequently easily form thermal stratification in warm seasons. Because of the deep water required for power generation, low temperature water was released downstream. In cold seasons, temperature differences become less as result of the mixing of water along the water column.

From Fig. 5, pH and DO in the water below the dam also are lower than that above the dam, but Ca^{2+} and Si concentrations show a reverse trend. The differences of pH, DO, Ca^{2+} and Si above and below the dam demonstrate that the influence of river damming on the downstream reaches are significant. Obviously, water quality shows a great discrepancy when river flow through a dam.

Generally, DO saturation in reservoir surface water is higher than that downstream of the dam. For example, in reservoir surface water, DO saturation can reach up to 126%, but its annual average value is only 60% in water downstream of the dam in the HY reservoir. Similarly, the pH of the surface water above the dam is higher than downstream water (Table 2). Obviously, water quality shows a great discrepancy when river flows through this dam. From Fig. 6, it is clear that the values of DO and pH decrease with the increase of water depth. Especially in the BH reservoir, bottom water had a quite low DO content.

The concentrations of Ca^{2+} and Si showed a reverse trend as compared to DO and pH. In Table 2, the two reservoirs with longer residence time (HF and HJD

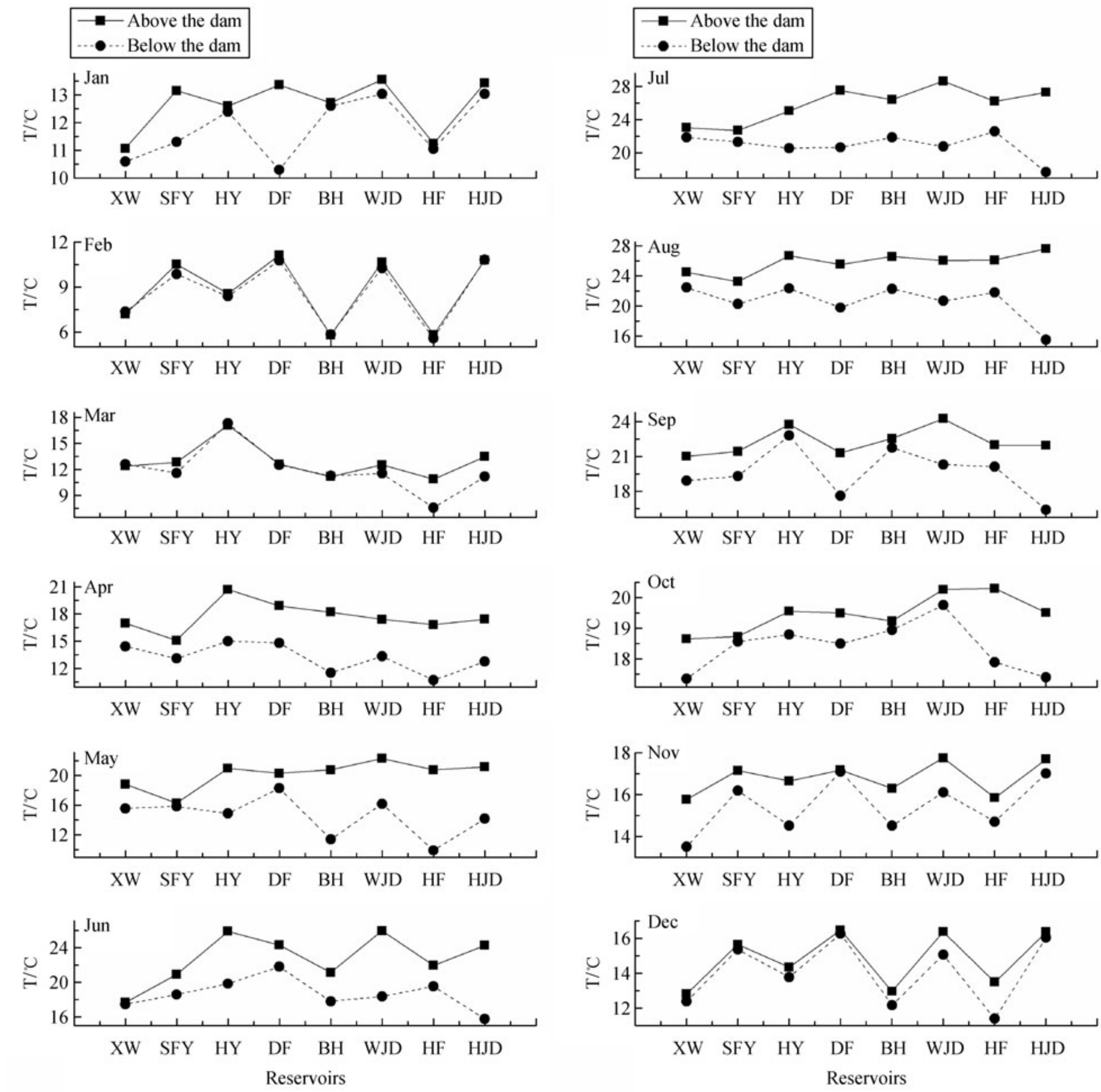

Fig. 4 Water temperature above and below the dam for 12 months (these reservoirs are arranged in *X* axes by residence time from short to long)

reservoirs) showed larger differences of Ca^{2+} and Si concentration between the surface water and the downstream water. There are two reasons for this phenomenon: (i) In reservoir surface water, during the growing season, dissolved silicon can be assimilated by diatoms, leading to the depletion of dissolved CO_2 in water and the resulting increasing of pH, which may increase *SIc* and favor the precipitation of $CaCO_3$. Both processes result in lower concentrations of Si and Ca^{2+} in reservoir surface water. (ii) The newly formed $CaCO_3$ and biomass will finally settle down into the reservoir sediment. Owing to organic matter decomposition, $CaCO_3$ and diatom frustules will be re-dissolved to some extent, and keep the high concentration of Ca^{2+} and Si in bottom water (Fig. 6). In reservoirs with longer residence time, the water column is easily forms thermal stratification in warm seasons. As a result, the exchange between the upper and bottom water is weak. Chemical stratification along the water column will then be maintained, consequently, such as in WJD, HJD, and HF reservoirs, while there is no obviously similar pattern in reservoirs with short residence time (Fig. 6). Furthermore, due to the deep water required for hydropower generation, water downstream of the dam has the similar chemical characteristics with the bottom water in the reservoir. Therefore, the river damming made an obvious difference of water chemical composition between the water

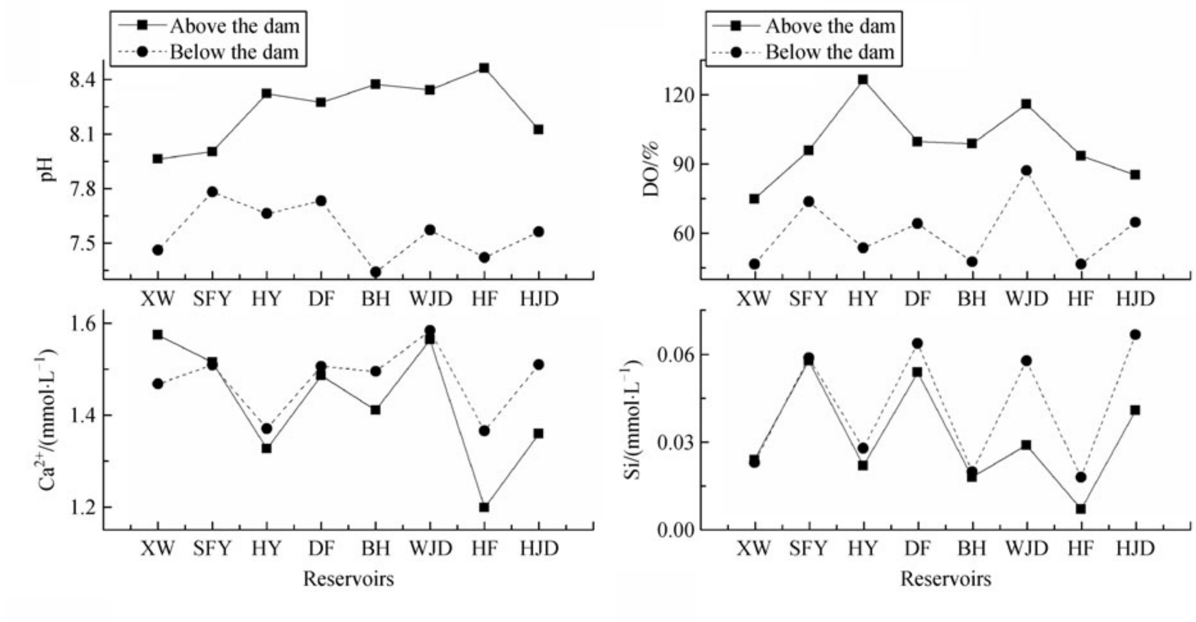

Fig. 5 pH, DO, Ca^{2+}, and Si (annual average value) above and below the dam (these reservoirs are arranged in *X* axes by residence time from short to long)

upstream and downstream of the dam, and influenced the calculation of the chemical weathering rate.

4.4 Influence of reservoirs in series on the carbonate equilibrium system of river water

SIc means the calcite saturation index. If $SIc > 0$, water is super saturated with respect to calcite, and calcium carbonate could deposit; if $SIc < 0$, water is under saturated with respect to calcite, and calcium carbonate dissolution could happen; and if $SIc = 0$, the system reaches equilibrium (Wang et al., 2011).

In the HF reservoir, which is about 40 km from its headwaters (Fig. 7), *SIc* is greater than zero in its reservoir surface water and less than zero in downstream water. This phenomenon also could be found in the BH, XW, and HY reservoirs. Due to the deep water discharging from the dam, the downstream *SIc* value inherited that of the bottom water of the reservoir. Figure 7 reveals that $CaCO_3$ precipitation is favored in surface water of a reservoir, while water downstream of the dam becomes erosive to $CaCO_3$, particularly in hot seasons. This great difference can be explained as follows: in reservoir surface water, during the growing season period, dissolved CO_2 could be significantly taken up by phytoplankton, leading to the increase of pH and *SIc*. As a result, $CaCO_3$ would precipitate. At the bottom of the reservoir, because of organic matter decomposition, CO_2 was released into water, which lowered the pH, and then decreased *SIc*. Under this condition, $CaCO_3$ re-dissolution will occur. In addition, reservoirs with longer retention time developed thermal stratification in hot seasons particularly, which lead to the exchange between the upper and lower water becoming weak. As a result, both Ca^{2+} and CO_3^{2-} concentrations can vary widely along the water column in these reservoirs. Figure 7 also shows the interception effect of reservoirs in series. From upstream of the leading reservoir (HF), the *SIc* in the water gradually increased; however, it reduced downstream of the reservoirs. In a word, the interception of reservoirs in series can disrupt the continuity of riverine chemical composition. Therefore, the interception effect of reservoirs in series should be considered when calculate the chemical weathering rate of a drainage basin.

5 Conclusions

River damming has obvious impact on water chemical composition, particularly in reservoirs with longer residence times. The geochemical behavior of conservative ions, such as Ca^{2+}, may become un-conservative when a river flows across a dam, because of changes in the carbonate equilibrium system.

Hydrological residence time of reservoirs has a certain relationship with the change of the water chemical composition, which may have some influences on the evaluation of chemical weathering rate. Due to the large number of reservoirs worldwide, these reservoirs may significantly change the original river characteristics. From the point of the whole basin and even the global chemical weathering rate, the influence of the reservoirs should

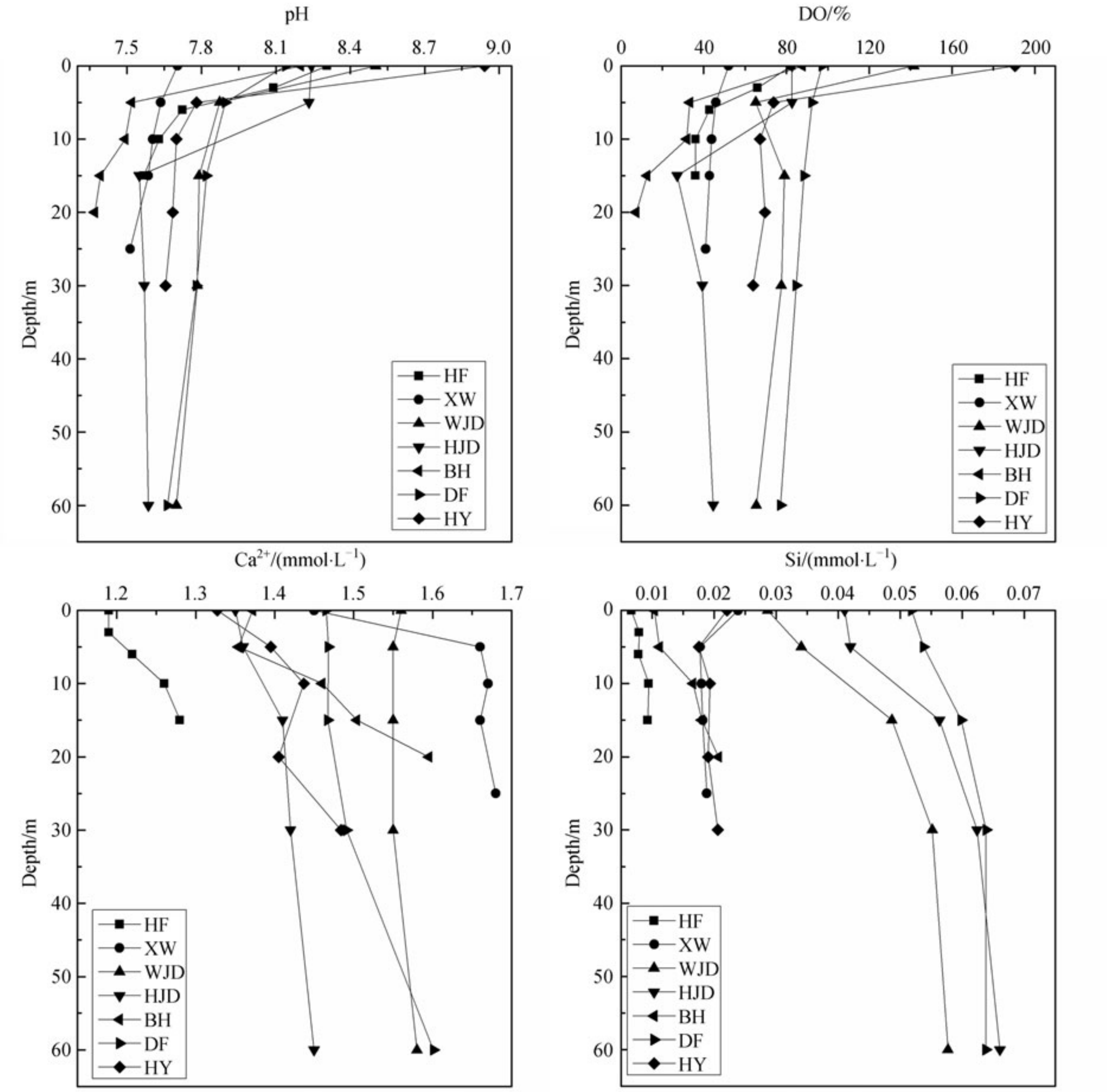

Fig. 6 Ca^{2+}, Si concentration and DO, pH (annual average value) profiles in reservoir

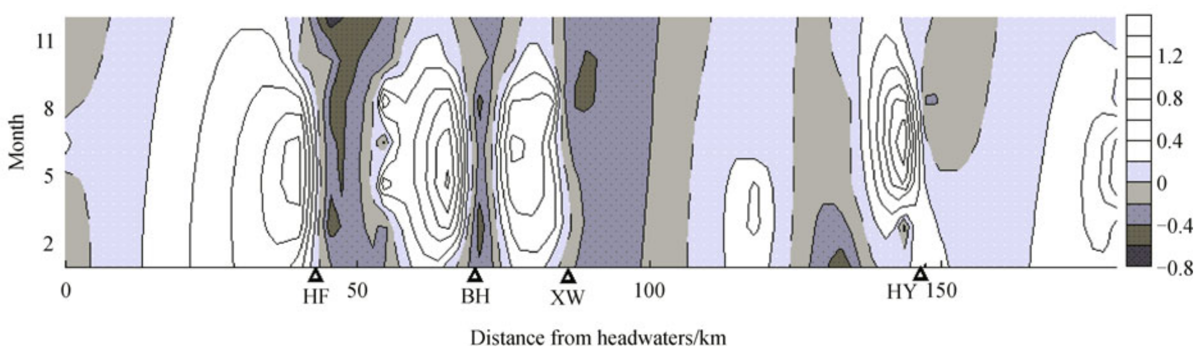

Fig. 7 $CaCO_3$ saturation index variation (The black triangle for the site of the dam)

not been ignored. Therefore, reservoir effect should be taken into account when calculating the CWR of drainage basins.

Acknowledgements The authors thank Huihui Li, Zhiwei Han, Chipeng Zhang, Yan Yang and Ganrong Li for their careful assistances in field sampling. This research was funded by the National Natural Science Foundation of China (Grant Nos. 41273128 and 40873066), and the Shanghai Education Committee Fund (12YZ017).

References

Brink J, Humborg C, Sahlberg J, Rahm L, Mörth M C (2007). Weathering rates and origin of inorganic carbon as influenced by river regulation in the boreal sub-arctic region of Sweden. Hydrol Earth Syst Sci Discuss, 4(2): 555–588

Cai Q H, Tang T, Liu J K (2003). Several hotspots in river ecology. Chinese J Appl Ecol, 14(9): 1573–1577 (in Chinese)

Chetelat B, Liu C Q, Zhao Z Q, Wang Q L, Li S L, Li J, Wang B L (2008). Geochemistry of the dissolved load of the Changjiang Basin rivers: anthropogenic impacts and chemical weathering. Geochim Cosmochim Acta, 72(17): 4254–4277

Draut A E, Logan J B, Mastin M C (2011). Channel evolution on the dammed Elwha River, Washington, USA. Geomorphology, 127(1–2): 71–87

Dumas D, Mietton M, Hamerlynck O, Pesneaud F, Kane A, Coly A, Duvail S, Baba M L O (2010). Large dams and uncertainties: the case of the Senegal River (West Africa). Soc Nat Resour, 23(11): 1108–1122

Dynesius M, Nilsson C (1994). Fragmentation and flow regulation of river systems in the northern third of the world. Science, 266(5186): 753–762

Han G L, Liu C Q (2004). Water geochemistry controlled by carbonate dissolution: a study of the river waters draining karst-dominated terrain, Guizhou Province, China. Chem Geol, 204(1–2): 1–21

Humborg C, Ittekkot V, Cociasu A, Bodungen B V (1997). Effect of Danue River dam on Black Sea biogeochemistry and ecosystem structure. Nature, 386(6623): 385–388

Jia J S, Yuan Y L, Zheng C Y, Ma Z L (2010). Dam construction in China: statistics, progresses and concerned issues. Water Power, 36 (1): 6–10 (in Chinese)

Kiss T, Fiala K, Sipos G (2008). Alterations of channel parameters in response to river regulation works since 1840 on the Lower Tisza River (Hungary). Geomorphology, 98(1–2): 96–110

Kummu M, Lu X X, Wang J J, Varis O (2010). Basin-wide sediment trapping efficiency of emerging reservoirs along the Mekong. Geomorphology, 119(3–4): 181–197

Li G R, Liu C Q, Chen C, Wang B L, Li J, Li S L, Liu X L, Wang F S (2009). Dissolve inorganic carbon and its carbon isotope composition in Cascade Reservoir of the Maotiao River during summer and autumn. Environ Sci, 30(10): 2891–2897 (in Chinese)

Mao Z P, Wang Y C, Peng W Q, Zhou H D (2005). Advances in effects of dams on river ecosystem. Advances in water science, 16(1): 134–140 (in Chinese)

Meybeck M (1982). Carbon, nitrogen, and phosphorus transport by world rivers. Am J Sci, 282(4): 401–450

Moquet J S, Crave A, Viers J, Seyler P, Armijos E, Bourrel L, Chavarri E, Lagane C, Laraque A, Casimiro W S L, Pombosa R, Noriega L, Vera A, Guyot J L (2011). Chemical weathering and atmospheric/soil CO_2 uptake in the Andean and Foreland Amazon basins. Chem Geol, 287(1–2): 1–26

Musil J, Horký P, Slavík O, Zbořil A, Horká P (2012). The response of the young of the year fish to river obstacles: Functional and numerical linkages between dams, weirs, fish habitat guilds and biotic integrity across large spatial scale. Ecol Indic, 23: 634–640

Qi J Y, Ruan X H (2005). Dam construction-induced environmental impact on riverine ecosystem. Journal of Hohai University, 33(1): 37–40 (Natural Sciences)

Walter R C, Merritts D J (2008). Natural streams and the legacy of water-powered mills. Science, 319(5861): 299–304

Wang F S, Wang B L, Liu C Q, Wang Y C, Guan J, Liu X L, Yu Y X (2011). Carbon dioxide emission from surface water in cascade reservoirseriver system on the Maotiao River, southwest of China. Atmos Environ, 45(23): 3827–3834

Wang S J, Yan Y X, Li Y K (2012). Spatial and temporal variations of suspended sediment deposition in the alluvial reach of the upper Yellow River from 1952 to 2007. Catena, 92: 30–37

Wu L, Huh Y, Qin J, Du G, van Der Lee S (2005). Chemical weathering in the Upper Huang He (Yellow River) draining the eastern Qinghai-Tibet Plateau. Geochim Cosmochim Acta, 69(22): 5279–5294

Wu W H, Xu S J, Yang J D, Yin H W (2008). Silicate weathering and CO_2 consumption deduced from the seven Chinese rivers originating in the Qinghai-Tibet Plateau. Chem Geol, 249(3–4): 307–320

Yang S L, Zhang J, Xu X J (2007). Influence of the Three Gorges Dam on downstream delivery of sediment and its environmental implications, Yangtze River. Geophys Res Lett, 34(10): L10401

Zhang Q, Singh V P, Chen X H (2012). Influence of Three Gorges Dam on streamflow and sediment load of the middle Yangtze River, China. Stochastic Environ Res Risk Assess, 25(4): 569–579

AUTHOR BIOGRAPHIES

Yang Gao is a Master at School of Environmental and Chemical Engineering, Shanghai University. He is mainly involved in the influence of the reservoirs for the rivers. E-mail: fengcui_xue@126.com

Fushun Wang is a Professor of School of Environmental and Chemical Engineering, Shanghai University. He is mainly engaged in reservoir environment effect and water environmental geochemistry. E-mail: fswang@shu.edu.cn